

Version: November 20, 2003, file name: physe2003(Machida, KF)ver2.doc

# **Dynamical simulation of phonon-assisted asymmetric transfer of photoexcited carriers in step-graded multiple quantum wells**

S. Machida, M. Matsuo and K. Fujiwara

Kyushu Institute of Technology, Tobata, Kitakyushu 804-8550, Japan

## Abstract

Dynamics of perpendicular motion of photoexcited electron-hole pairs assisted by phonon scattering is investigated by a rate equation analysis in a novel step-graded staircase  $\text{In}_x(\text{Al}_{0.17}\text{Ga}_{0.83})_{1-x}\text{As}$  multiple quantum well heterostructure. When there exist built-in potential gradients in the heterostructure by changing the In mole fraction ( $x$ ) in each well, those carriers that are thermally released by the particular well move unidirectionally from shallower to deeper wells. That is, asymmetric unidirectional motion of photoexcited carriers is realized via phonon-assisted activation above the barrier band edge state. This perpendicular motion of carriers was measured by monitoring the transient photoluminescence (PL) signals, which are spectrally discriminated between the wells. The PL dynamics is rigorously and quantitatively explained based on the dynamical simulation as a function of temperature using extracted parameters of the recombination and transfer times.

PACS: 78.66.Fd; 78.47.+p; 78.55.Cr; 73.63.Hs

*Keywords:* Photoluminescence; III-V semiconductor; Quantum well; Vertical transport

---

Corresponding author. Telefax: +81-93-884-3221;  
*E-mail address:* [fujiwara@ele.kyutech.ac.jp](mailto:fujiwara@ele.kyutech.ac.jp) (K. Fujiwara)

## 1. Introduction

When carriers are placed in a semiconductor heterostructure with built-in potential gradients, they can undergo perpendicular motion or inversely motion is blocked for enhancing the stimulated emission [1]. This type of directional transport control in sophisticated quantum heterostructures [2] is recently becoming more and more important for device applications such as intersubband quantum cascade lasers [3]. In relation to control of the perpendicular transport, unique phenomena of dynamical increases of the photoluminescence (PL) intensity at higher lattice temperatures have recently been observed due to the perpendicular cascading of photoexcited carriers in a novel step-graded quantum well (QW) heterostructure [4,5]. In this paper, the dynamics of perpendicular motion of photoexcited electron-hole pairs assisted by phonon scattering is investigated by a rate equation analysis in the step-graded staircase QW heterostructure. Our simulation of PL dynamics rigorously proves the asymmetric perpendicular flow of photoexcited carriers and capture by the deeper QW.

## 2. Experimental and theoretical

The sample used for the present study consists of strained  $\text{In}_x(\text{Al}_{0.17}\text{Ga}_{0.83})_{1-x}\text{As}$  multiple QWs with similar widths of about 8 nm, but with five different  $x$  values (5.3, 8.8, 12, 15 and 18%, named QW1, 2, 3, 4 and 5, respectively), which are electronically isolated by 30 nm thick  $\text{Al}_{0.17}\text{Ga}_{0.83}\text{As}$  barriers [6]. Previous results [4] of the temperature dependence of cw PL spectra reveal five distinct peaks corresponding to the five QW layers, which are spectrally well discriminated and dramatically evolve with increasing lattice temperature. As the temperature increases, some of the PL peaks first

increase their relative intensities in the intermediate temperature range and then decrease the signal amplitudes progressively from shorter wavelength sides. These changes of the PL intensities as a function of temperature reflect that the photoexcited carriers unidirectionally move from shallower to deeper QWs via phonon-assisted activation above the barrier band edge state. PL transients by measuring spectral- and time-resolved PL signals using a streak camera system [5] directly evidence the perpendicular flow of photoexcited carriers and capture by the deeper QW, providing firm evidences for the carrier flow and capture processes.

In order to better understand the PL dynamics by simulating the transient PL signals, rate equations for the occupation number of the five wells are numerical solved for the model potential structure of electron-hole pairs as shown in Fig. 1. Depth of the potential well ( $\Delta E_i$  for the  $i$ -th well) for electron-hole pairs is estimated from difference between the energy gap ( $E_g = 1.7566$  eV) for  $\text{Al}_{0.17}\text{Ga}_{0.83}\text{As}$  barriers and PL peak energy ( $E_{\text{PL}i}$ ) [6], as summarized in Table 1 of Ref. [5]. Thermal activation energy ( $k_B T$ ) is estimated from temperature at which carriers start to escape from the particular well based on the PL results [4,5]. Ratios of the parameters of  $\Delta E_i$  coincide with those of  $k_B T$  (T) at least for QW2, QW3 and QW4. This result indicates that the claimed carrier transport mechanism is justified in terms of thermal activation for the five QWs.

To simulate the PL dynamics, we have made numerical calculations of the five-components rate equation for the exciton or electron-hole pair occupation number  $N_i$  ( $i = 1, 2, 3, 4$  and  $5$ ) in QW1, QW2, QW3, QW4 and QW5, respectively, as sketched in Fig. 1. Assuming ratios of the carrier generation rate  $r_i$  in QW $i$  by direct laser excitation (generation function is defined as  $G(t)$ ), these five rate equations are given by,

$$\frac{dN_1}{dt} = r_1 G(t) - \frac{N_1}{\tau_{r1}} - \frac{N_1}{\tau_{nr}} - \frac{N_1}{\tau_{12}}, \quad (1)$$

$$\frac{dN_i}{dt} = r_i G(t) + \frac{N_{i-1}}{\tau_{i-1i}} - \frac{N_i}{\tau_{ri}} - \frac{N_i}{\tau_{nr}} - \frac{N_i}{\tau_{i+1i}} \quad (i = 2 - 4), \quad (2)$$

$$\frac{dN_5}{dt} = r_5 G(t) + \frac{N_4}{\tau_{45}} - \frac{N_5}{\tau_{r5}} - \frac{N_5}{\tau_{nr}}. \quad (3)$$

For the calculations, we take into account of the radiative ( $\tau_{ri}$ ) and non-radiative ( $\tau_{nr}$ ) recombination times and the transfer time  $\tau_{ij}$  from the  $i$ -th well to the neighboring  $j$ -th well at the lower potential side. It is worth to note here that we only need to use a single non-radiative lifetime ( $\tau_{nr}$ ) due to the common  $\text{Al}_{0.17}\text{Ga}_{0.83}\text{As}$  barriers at a fixed lattice temperature, while the five radiative recombination times ( $\tau_{ri}$ ) that are approximately linearly dependent on temperature are assumed [7]. We treat these characteristic time constants as adjustable parameters, which are all temperature-dependent. For calculational simplicity, we assume that the carrier transfer beyond the nearest neighbor wells can be neglected. We also assume that the carrier generation in each well by laser excitation is fast enough, neglecting the initial energy relaxation processes from the barrier state. Using the transient population  $N_i(t)$  numerically calculated, the PL transient,  $I_{\text{PL}}^i(t)$  is determined by the equation,  $I_{\text{PL}}^i(t) = N_i(t)/\tau_{ri}$ . These procedures allow us to almost perfectly fit the PL transients for the five emission bands as described in the followings.

### 3. Results and discussion

Simulation results (by solid curves) together with the experimental PL transients are plotted in Figs. 2 (a), (b) and (c) (for QW2, QW3 and QW4, respectively) at temperatures of 12, 20, 30, 40, 50,

70 and 90 K. Both of the wavelength-integrated PL intensity and time behaviors are all well reproduced in Fig. 2, assuming almost linear temperature dependence of  $\tau_{r1}$  and decreased  $\tau_{nr}$  values with temperature. Specifically, the PL time behaviors of QW2, QW3 and QW4 in Fig. 2 are basically determined by radiative recombination times of free and localized excitons between 12 and 40 K. The initial increases of the PL decay time with temperature for QW2, QW3 and QW4 can easily be understood in terms of the temperature-dependent radiative recombination rate of free excitons in QW [7], while the decreases of the PL intensity with temperature are ascribed to the thermal activation of non-radiative recombination centers. Parameters of the radiative recombination times and the non-radiative recombination time used for the simulation are plotted in Fig. 3 (a), while the transfer times between the neighboring QWs are shown in Fig. 3 (b). The radiative recombination times in Fig. 3 (a) decrease with increasing the potential well depth ( $\Delta E_i$ ) at any temperature due to the increased quantum confinement of carriers. The radiative recombination times assumed for the simulation are thus consistent with the trends theoretically expected for the excitonic transition [7] in order to quantitatively fit the PL transients for each QW as a function of temperature.

However, an important observation to be stressed here is that a significant increase of the PL rise accompanying the drastic PL intensity enhancement is clearly observed when the temperature is further increased to 50 K in Fig. 2 (b) for QW3. This recovery of the PL intensity and the appearance of PL rise are unique in this type of stepped QW sample, and provide a firm evidence for the carrier flow and capture processes assisted by phonon scattering. At 50 K, we note that, when the PL intensity of QW3 is significantly increased, a faster PL decay (quenching) of the neighboring shallow QW2 is observed in Fig. 2 (a), which verifies the carrier escape from QW2 to QW3. When the

temperature is furthermore increased to 70 K, the PL decay of QW3 becomes even faster with a decay time constant of 1.1 ns as seen in Fig. 2 (b), revealing the transfer of carriers to the deeper neighboring QW4. The increase of the PL intensity at 50 and 70 K for QW4, especially at later times in Fig. 2 (c) reflects the transfer of carriers to the QW4 from QW3, although the initial PL intensity at 0-0.6 ns is lower due to the non-radiative processes at 70 K. At 90 K the PL intensity for QW3 is very quickly quenched by completely transferring to the deeper QW4 and QW5. Most of the transferred carriers are however trapped at this temperature by non-radiative recombination centers, since the non-radiative recombination time is shorter than  $\tau_{\text{r}}$  except for QW5 (see Fig. 3 (a)). Thus, the reduced PL intensities are observed (see also Fig. 3 of Ref. [4]). These simulation results of PL transients clearly and directly demonstrate the dynamical carrier flow and capture processes between the different QW layers. The carrier motion is always from the shallower to the deeper well with the higher In mole fraction, so that the transfer time  $\tau_{ij}$  in Fig. 3 (b) progressively increases as the depth of the escaping well becomes deeper. This can be easily understood in terms of the higher order phonon scattering processes involved for such deeper well. We note that, when the transfer time between the neighboring QWs becomes comparable to or shorter than the radiative recombination lifetime of a shallower well (see Fig. 3), the PL intensity as well as the PL decay time drastically decreases. That is, the PL recombination dynamics is basically determined by interplay of the radiative recombination and carrier transfer times. Thus, our theoretical studies of the PL dynamics directly confirm the perpendicular flow of photoexcited carriers and capture by the deeper QW.

#### 4. Conclusion

Dynamics of perpendicular motion of photoexcited electron-hole pairs assisted by phonon scattering is investigated by a rate equation analysis in a novel five-steps staircase QW heterostructure. The simulation results by numerically solving the five-components rate equation for the electron-hole pair occupation number in the five QWs reproduce well both of the PL intensity and time behaviors, assuming almost linear-temperature dependence of radiative lifetimes and a common non-radiative lifetime decreasing with temperature. Thus, unidirectional phonon-assisted asymmetric transfer of photoexcited carriers is dynamically observed in the novel stepped QW heterostructure. These simulation results indicate that a design of stepped heterostructures can be actually used to tailor directional motion of carriers in QW heterostructures.

### **Acknowledgement**

The authors would like to thank J. R. Folkenberg and J. M. Hvam for providing the sample used for the present study and K. Satoh, T. Nogami, and A. Satake for their experimental assistance and useful comments on the rate equation analysis.

## References

- [1] H. Krömer, *Rev. Mod. Phys.* 73 (2001) 783.
- [2] H. T. Grahn (Ed.), *Semiconductor Superlattices: Growth and Electronic Properties* (World Scientific, Singapore, 1995).
- [3] J. Faist, F. Capasso, D. L. Sivco, C. Sirtori, A. L. Hutchinson, A. Y. Cho, *Science* 264 (1994) 553.
- [4] S. Machida, M. Matsuo, K. Fujiwara, J. R. Jensen, J. M. Hvam, *Physica E* 13 (2002) 182.
- [5] S. Machida, M. Matsuo, K. Fujiwara, J. R. Folkenberg, J. M. Hvam, *Phys. Rev. B* 67 (2003) 205322.
- [6] J. R. Jensen, J. M. Hvam, W. Langbein, *J. Appl. Phys.* 86 (1999) 2584.
- [7] J. Feldmann, G. Peter, E. O. Göbel, P. Dowson, K. Moore, C. Foxon, R. J. Elliott, *Phys. Rev. Lett.* 59 (1987) 2337.



## Captions to Figures

**Fig. 1** Calculation model for carrier transfer assisted by phonon scattering between the five quantum wells with different potential depths.

**Fig. 2** Semi-logarithmic plots of the simulated PL intensity (smooth solid curves) and the experimental results (solid and dotted curves) (a) for QW2 at 12, 20, 30, 40, 50 and 70 K, (b) for QW3 at 12, 20, 30, 40, 50, 70 and 90 K and (c) for QW4 at 12, 20, 30, 40, 50, 70 and 90 K. The laser excitation pulse is located at 0.0 ns in the ordinate of this figure.

**Fig. 3** Parameters used for simulation of (a) radiative and non-radiative recombination times and (b) transfer times as a function of temperature.

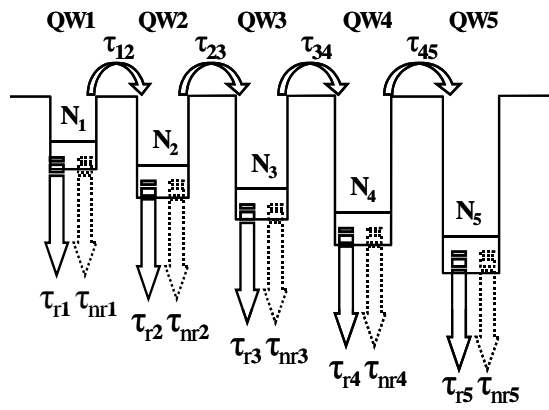


Fig. 1

Physica E

Machida et al

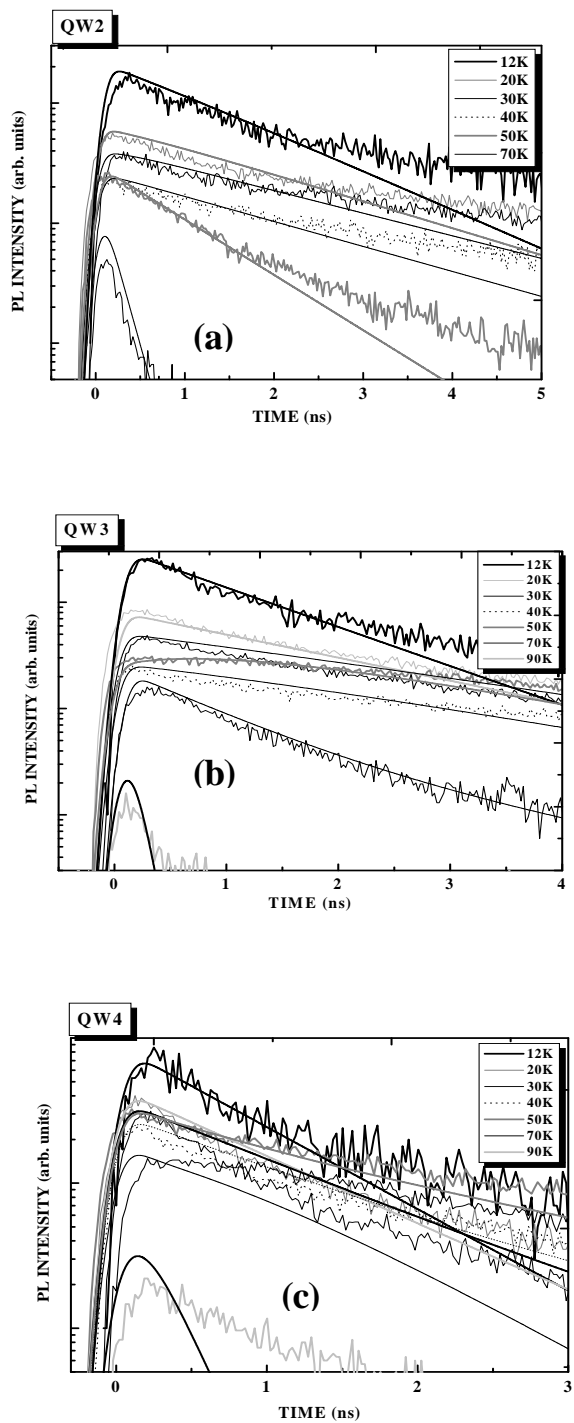


Fig. 2

Physica E

Machida et al

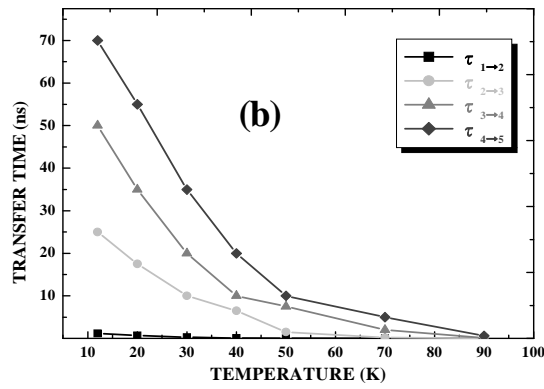
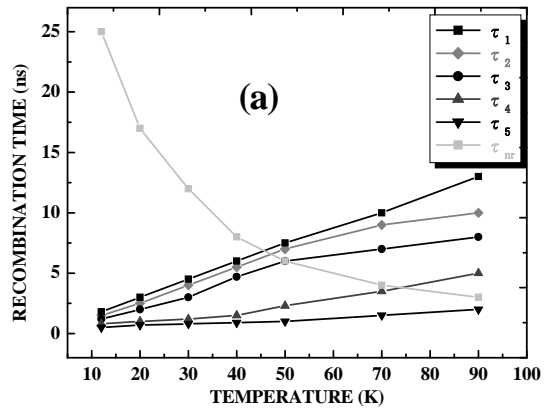


Fig. 3

Physica E

Machida et al